Development of radiographic chest phantoms[a)]

Chris Constantinou,[b)] John Cameron, Larry DeWerd, and Margaret Liss
Midwest Center for Radiological Physics, University of Wisconsin, Medical Physics Department, Madison, Wisconsin 53706

(Received 3 December 1984; accepted for publication 27 January 1986)

Diagnostic imaging studies, particularly in chest radiography, require adequate phantoms. Two such phantoms have been made and used; one is a semianthropomorphic phantom and the other is a geometric phantom with embedded test objects. These phantoms, constructed of epoxy resin-based solid water, are described in detail and compared to a common commercial phantom.

I. INTRODUCTION

The need for a quality control program in diagnostic radiology has been emphasized in the past.[1] Such a program is of particular importance in chest radiography, since this examination comprises a significant portion of all medical x-ray examinations each year. One of the most important tools required for a good quality control program is a suitable phantom. High-contrast resolution, low-contrast detectability, film latitude, magnification, alignment/centering, and phototimer performance of chest x-ray systems are some of the parameters that have to be evaluated quantitatively and routinely. For these evaluations, a simple geometric phantom with appropriate test pieces embedded in it is adequate. However, studies for technique optimization, patient simulation, and observer performance require a more sophisticated anthropomorphic phantom and a realistic radiographic appearance.

Constructing such a phantom to simulate the chest is technically difficult. The phantom must be made of materials that are tissue equivalent so that the phantom image is representative of clinical conditions, but any biological tissue (fixed real lungs, etc.) embedded in the phantom will differ from specimen to specimen and may not be stable over a period of time.

Christensen *et al.*[2] developed a modular chest phantom consisting of several drawers with 1-cm-thick Lucite walls and approximate dimensions 30×35 cm. Each drawer contained one component, for example, a heart made of wax, human ribs cut to size, inflated and fixed lung from a dog, etc. This phantom was used to investigate the effect of quantum mottle on the detection of pulmonary disease.

Pearce *et al.*[3] produced a phantom with a more realistic shape, which included lung vascular structures and simulated pathological conditions; a commercial version of this phantom is available.[4] They used a thoracic skeleton embedded in Plexiglas with the addition of inflated, formalin-fixed dog lungs which they impregnated by hand with latex rubber until the subpleural vessels were visible. The lungs and rubber-based mediastinum were inserted into the thoracic cage and the remaining space was filled with urethane foam. Since the lung and mediastinum complexes are removable and interchangeable, it is possible to create and compare different pathological conditions with such a phantom. Other non-anthropomorphic chest phantoms used in the past have been developed by the American National Standards Institute[5] and the Bureau of Radiological Health.[6]

In an attempt to produce a more versatile radiographic chest phantom, the Midwest Center for Radiological Physics (MWCRP) developed two phantoms designed to satisfy different goals. The first (semianthropomorphic) phantom was designed for patient simulation and may be used for quality assurance of chest x-ray units, as research and teaching, intercomparison of images, screen–film systems, etc; the second (geometric) phantom is useful for imaging and quality control tests and for testing the phototimer performance of automatic chest x-ray units.

II. MATERIALS AND METHODS

Both phantoms are made from "solid water" (WT/SR1),[7] an epoxy resin-based material which has attenuation and energy absorption coefficients within 1% of those for liquid water in the energy range from 10 keV to 100 MeV and within 4% of those for muscle in the same energy range.[7,8]

A. Semianthropomorphic phantom

The four-layer semianthropomorphic phantom consists

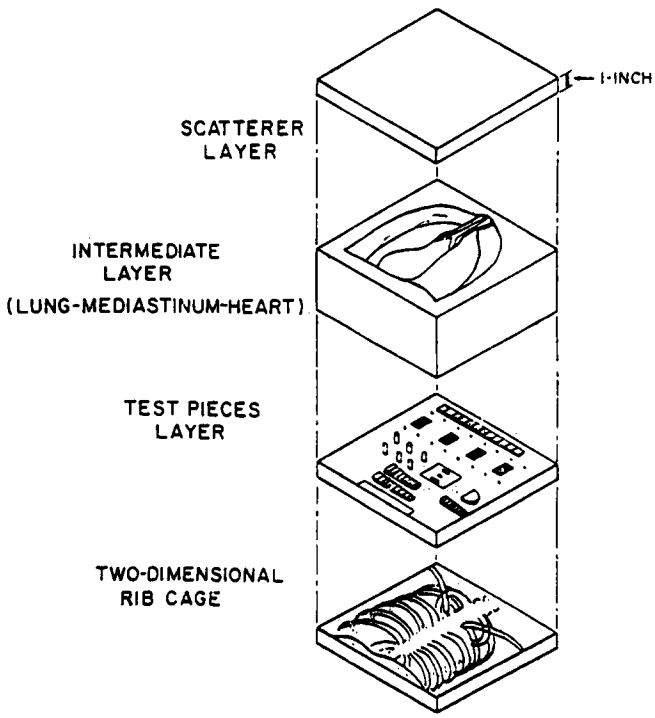

FIG. 1. Schematic diagram of semianthropomorphic chest phantom.

 0094-2405/86/060917-05$01.20

TABLE I. Average film densities of ten radiographs of the semianthropomorphic phantom and real human chests measured at the same specific position. The images, made at 85 and 115 kVp, were phototimed. Numbers in parentheses indicate standard deviation.

Position	Semianthropomorphic phantom	Human chest
Base + fog	0.21 (0.01)	0.22 (0.01)
Lung region between fifth and sixth ribs	1.76 (0.43)	1.72 (0.42)
Under shadow of fourth rib in lung region	1.66 (0.48)	1.59 (0.48)
1 cm below the top edge of the diaphragm	0.45 (0.12)	0.54 (0.26)

of (1) a layer containing various test pieces, (2) a layer representing the thorax and mediastinum, (3) an aluminum and Lucite layer representing a two-dimensional projection of the rib cage, and (4) a scatter layer (Fig. 1). The overall dimensions of the phantom are $35 \times 35 \times 20$ cm. The dimensions were chosen on the basis of optical density measurements of radiographs of an "average" human chest. The thickness of the patients whose radiographs were chosen varied between 23 and 25 cm. The radiographs were chosen by a radiologist and optical density measurements were made at the points shown in Table I. The thickness of the phantom at each of these points was adjusted so as to achieve the same optical densities on radiographs of the phantom using the same exposure techniques as for humans.

The "solid water" layer simulating the thoracic cavity and mediastinum has realistic representations of the heart, trachea, and bronchi. Lung nodules and other pathological structures can be added; the detectability of these pathological structures can be tested with and without extra scatter material. Figures 2(a) and 2(b) show radiographs of a human chest and the semianthropomorphic chest phantom, respectively, taken with 115-kVp phototimed exposures; other test radiographs were made at up to 140 kVp.

The layer with the test pieces was designed to test for high-contrast resolution, low-contrast detectability, and film latitude. It contains wire meshes (from 0.8 to 4 holes/mm), aluminum oxide spheres of 0.6, 1.0, and 1.6 mm in diameter, and a lead bar pattern. Bone substitute (SB3)[9] and Lucite step wedges, as well as simulated fat substitute (FT/SF1)[7] cylinders, were included for measurement of radiographic contrast and film latitude. The step wedges were imaged in both the diaphragm and the lung regions. This allowed a comparison of optical density differences between any two given steps in low- and high-density regions. Specks of Al_2O_3 with dimensions between 0.75 and 1.0 mm on the steps of an aluminum step wedge with step thicknesses from 1 to 12 mm show the effect of reduced contrast on resolution. Three sets of cylinders (Teflon, Lucite, and nylon) of height equal to their diameter, ranging from 3 to 19 mm, test the detectability of high-contrast, medium-contrast, and low-contrast objects, respectively. Figure 3 shows an x-ray image of the test layer taken at 80 kVp to show the included test objects; this layer can also be used with the geometric phantom (see below).

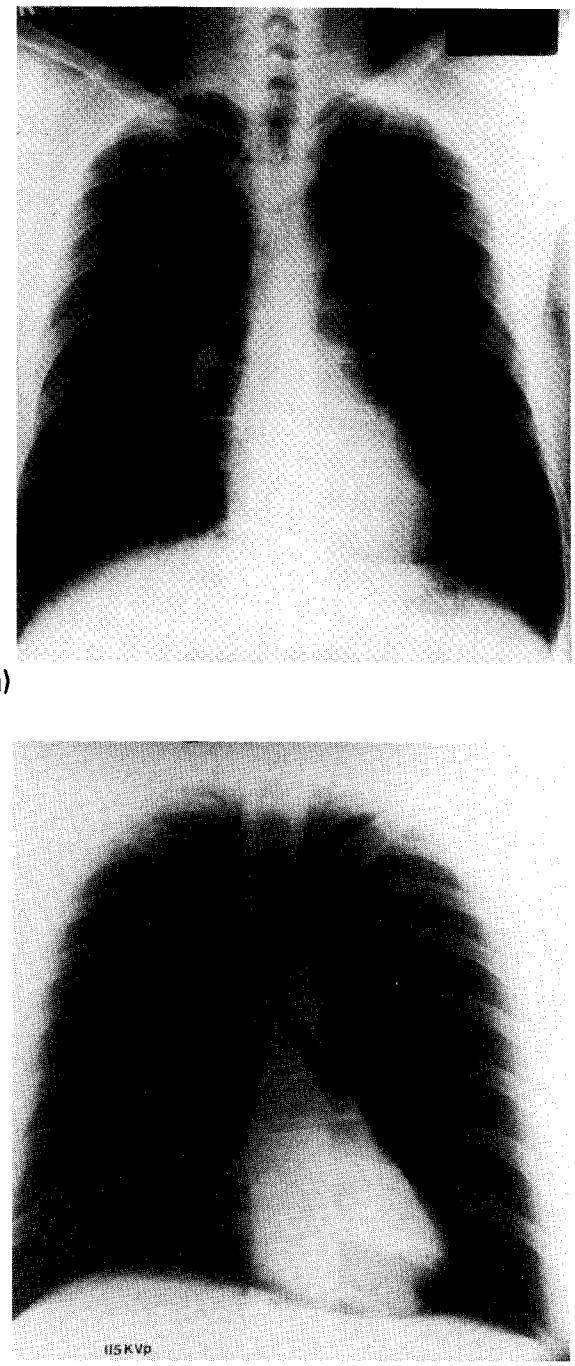

(a)

(b)

FIG. 2. Radiographs of (a) normal human chest and (b) the semianthropomorphic phantom (115 kVp).

The third layer consists of a two-dimensional projection of the rib cage, made of 2-mm-thick aluminum glued onto a 1-cm-thick "solid water" plate. Additional 2.5-cm-thick layers can be used with the phantom to simulate average and thicker patients, respectively. The additional layers can be used in conjunction with the rib cage and mediastinum structures to show the effect of extra scatter on resolution

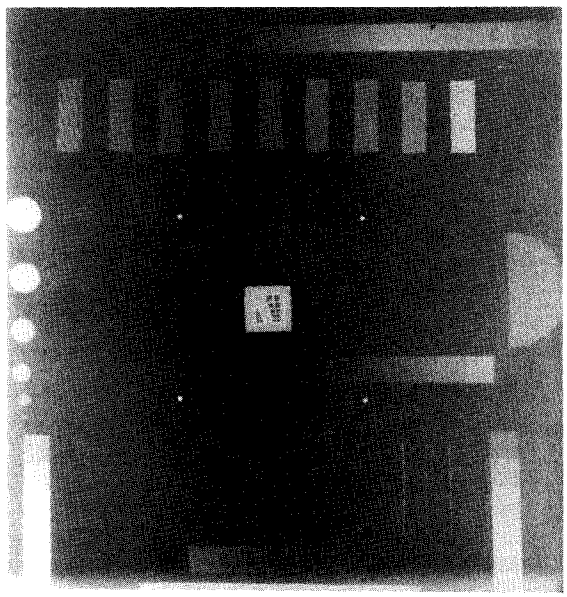

FIG. 3. Radiograph of the "test pieces layer" of the semianthropomorphic chest phantom.

and detectability of low-contrast nodules. An effort was made to reproduce blood vessels using rod-like solid-water mix, with unsatisfactory results.

B. Geometric phantom

The simple geometric phantom consists of three slabs: two plain slabs $30 \times 30 \times 2$ cm and a 6-cm-thick slab containing test pieces similar to those described above. The test objects in the geometric phantom [Fig. 4(a)] are used to measure resolution, low-contrast detectability, and film latitude. Many of the test objects are modeled after those reported elsewhere by one of the authors.[7] The test pieces include a simulated bone step wedge with five steps of thicknesses from 0.5 to 2.5 cm, and an air step wedge with five steps of thicknesses from 1 to 5 cm. These steps were designed to cover optical densities ranging from 0.5 to 1.5. The bone step wedge tests the response of the system to high-density structures in the chest; the air step wedge is used to test the ability to detect the presence of gas collections within soft tissue. A hemispherical and a cylindrical (1-cm-diam) nodule of solid water have been cast on each step of the air wedge, for studies of detectability of lung nodules with varying film density. Six Lucite cylinders with diameters equal to their height, ranging from 3 to 19 mm, are useful for establishing the smallest "medium-contrast" object that can be detected at various kVp and mAs values. Aluminum oxide specks of 1.0 and 1.5 mm in size are used for high-contrast resolution tests. The effect of varying the concentration of contrast solutions in simulated blood vessels can be studied with the help of four sets of Teflon tubes filled with 12.5%, 25%, 50%, and 100% iodine contrast solution. Each set is comprised of three tubes with internal diameters of 0.3, 0.7, and 1.35 mm. A $3 \times 2 \times 0.2$ cm lead piece shields the film to permit "base plus fog" density readings on the film. All the above objects are placed along the edges while the central area (20×20 cm) is left clear for phototimer linearity checks. The simulated

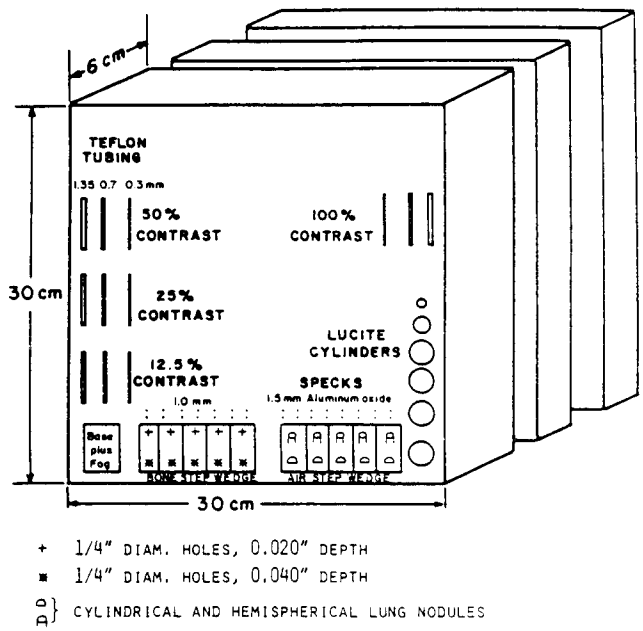

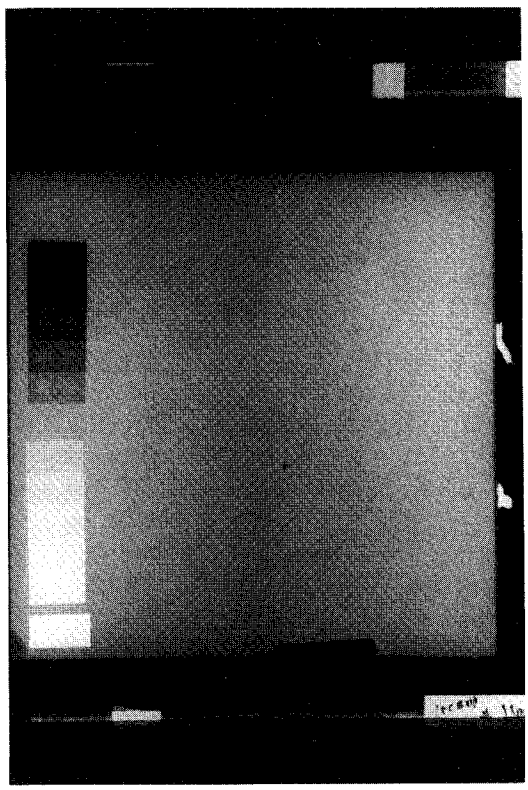

FIG. 4. The geometric phantom: (a) schematic diagram of the geometric phantom used for phototimer performance and routine quality control tests; and (b) radiograph of the geometric phantom (100 kVp).

blood vessels and the air step wedge are modeled after those in a commercially available phantom.[10] Figure 4(b) shows a radiograph of the geometric phantom taken with a 100-kVp setting on a phototimed unit.

III. RESULTS

The phantoms were tested on a number of different chest x-ray units. Lucite cylinders of height and diameter equal to

TABLE II. Comparison of entrance exposures measured on the surface of three different phantoms and a typical patient.

Phantom or patient	kVp	PA entrance skin exposure (mR)
Semianthropomorphic phantom[a]	100	23
	120	22
	140	22
Humanoid (Ref. 4)	100	20
	120	19
	140	19
Geometric phantom[b]	100	20
	120	18
	140	17
Real patient: (23-cm chest) (TLD-100 measurement)	140	22

[a] Consists of intermediate layer which includes heart, mediastinum and lungs, aluminum skeleton, and 5 cm of scatter layer.
[b] Consists of the 6-cm-thick layer which contains test pieces and two 2.0-cm-thick unit-density layers.

12.5 mm or larger were seen if the test layer was radiographed alone, but none of the cylinders were visible when scatter from the rest of the semianthropomorphic phantom was added. When the additional layers were added, the 19-mm nylon cylinder was not visible and the 1-mm aluminum oxide specks on the aluminum step wedge were difficult to visualize. This shows the significant effect of reduced contrast on the detectability of various objects. The mAs value for phototimed postero–anterior (PA) exposures of human chests, with patient thicknesses from 17 to 24 cm, and a range of 115–125 kVp were similar to those obtained with both phantoms with appropriate scatter material.

Densities observed at selected points on PA human chest radiographs taken at various kVp settings were compared with the average densities at corresponding points on phototimed radiographs of the semianthropomorphic phantom. The range of densities observed on radiographs of humans is similar to those on the phantom radiographs (Table I).

Table II shows a comparison of average "skin" or entrance exposures measured with an ion chamber for three different phantoms. The real patient exposure measurements were made with TLD-100 thermoluminescent dosimeters, using the same phototimed chest x-ray unit. It can be seen that the exposures vary from 17 to 23 mR depending on the kVp used. The exposures measured with the geometric phantom are slightly lower indicating that the thickness of unit-density material required to match the equivalent thickness of the "average" chest is closer to 12 cm, instead of the 10-cm total thickness used with the geometric phantom.

IV. DISCUSSION

The semianthropomorphic phantom could be further refined. Instead of the aluminum two-dimensional projection of the rib cage, it would be desirable to make molds and produce realistic three-dimensional rib cages using epoxy resin-based bone substitute materials. This is feasible but time consuming and expensive. Molds for some vertebrae have been produced and realistically shaped vertebrae have been made. Also, the production of the pattern produced by the lung vasculature is difficult to simulate and presents serious problems. Epoxy resin-based foamed lung[7] appears as diseased lung on radiographs and, although its attenuation is adequate, the image is not clinically acceptable. Real dog lungs fixed with chemicals in the inflated state and impregnated with solid materials simulating blood have been employed[4] with reasonable but not completely adequate results because small blood vessels are not preserved. The semianthropomorphic phantom can be used with the lung cavity left unfilled, producing acceptable results. Conceptually, it would be desirable to be able to insert other disease simulations for diagnostic tests. However, the construction of an ideal anthropomorphic chest phantom, which would reproduce human chest radiographs containing all the detailed lung vasculature, is very difficult.

The advantages of this phantom are: (1) it circumvents the scarcity of human skeletons and the difficulty in preserving animal lungs and hearts; (2) it can be manufactured using simulated water[7–9]; (3) the thickness can be varied so as to enable evaluation of phototimer performance; (4) the geometric phantom has standard test objects for evaluation of radiographic performance; and (5) radiographic images of phantoms made in this manner can be intercompared because of the high reproducibility of the phantoms.

The geometric phantom appears adequate for some quality control procedures and for testing the performance of phototimed units. The exposures necessary for this phantom are slightly lower than for human radiographs. This can be compensated for by the addition of extra scattering material.

Although the radiographic images of step wedges and Lucite or Teflon beads bear no resemblance to anatomical structures found in radiographs of the human body, their inclusion as test objects provides useful information on machine related imaging parameters. Both phantoms described in this paper could be used in intercomparisons of equipment and techniques.

ACKNOWLEDGMENTS

We thank Dr. Albert Alter for his help in film evaluation, and Radiation Measurements Incorporated, Middleton, WI, for the use of their facilities to make the phantoms.

This project has been funded in part by the National Cancer Institute under Contract No. N01-CN-05504.

[a] Commercial product identification does not imply a recommendation or endorsement by the authors or their institutions, nor does it imply that they consider the identified product to be the best available for the purpose.
[b] Present address: Tufts University School of Medicine, New England Medical Center, Department of Therapeutic Radiology, 171 Harrison Avenue Boston, MA 02111.

[1] Bureau of Radiological Health, "Quality Assurance for Radiographic X-Ray Units and Associated Equipment," HEW Publ. (FDA) No. 79-8094 (1979).
[2] E. E. Christensen, G. W. Dietz, R. C. Murry, and J. G. Moore, in Proceedings of a Symposium on Optimization of Chest Radiography, Madison, WI, HHS Publ. (FDA) No. 80-8124, 1980, p. 249.

[3]J. G. Pearce, G. Gillan, W. Roeck, in Proceedings of a Symposium on Optimization of Chest Radiography, Madison, WI, HHS Publ. (FDA) No. 80-8124 1980, p. 255.
[4]Humanoid Systems, Inc., Carson, CA 90746.
[5]P. A. Arimilli, "ANSI Standards" in *The Physics of Medical Imaging: Recording System Measurements and Techniques*, AAPM Monograph No. 3, edited by A. G. Haus (American Institute of Physics, New York, 1979,) p. 105; also, "Method for the Sensitometry of Medical X-Ray Screen–Film Processing Systems," Am. Natl. Stand. Inst. Publ. No. PH2.43-1982, 1982.
[6]B. J. Conway, P. F. Butler, J. E. Duff, T. R. Fewell, R. E. Gross, R. J. Jennings, G. H. Kustenis, J. L. McCrohan, F. G. Rueter, and C. K. Showalter, Med. Phys. **11**, 827 (1984).
[7]C. Constantinou, Ph.D. thesis (London University, 1978).
[8]C. Constantinou, F. H. Attix, and B. Paliwal, Med. Phys. **9**, 436 (1982).
[9]D. R. White, Med. Phys. **5**, 467 (1978).
[10]Model No. 170 chest radiographic phantom, Radiation Measurements, Inc., Middleton, WI 53562.